IMAGE ANALYSIS AND SEGMENTATION IN ADOBE PHOTOSHOP FOR QUANTIFICATION OF INTRAPULMONARY ARTERIOVENOUS SHUNTING AT VARIOUS LEVELS OF ACUTE HYPOXIC EXPOSURE

By

KARA MARIE BEASLEY

A THESIS

Presented to the Department of Human Physiology
And the Honors College of the University of Oregon
In partial fulfillment of the requirements
For the degree of Bachelor of Science

June 2009

Abstract of the thesis of

Kara Marie Beasley for the degree of Bachelor of Science

In the Department of Human Physiology to be taken June 4, 2009

Title: IMAGE ANALYSIS AND SEGMENTATION IN ADOBE PHOTOSHOP FOR QUANTIFICATION OF INTRAPULMONARY ARTERIOVENOUS SHUNTING AT VARIOUS LEVELS OF ACUTE HYPOXIC EXPOSURE

Approved:_____

Andrew Lovering, PhD

It was hypothesized that intrapulmonary arteriovenous (IPAV) shunt pathways would be recruited at rest under various levels of acute hypoxic exposure. Thirteen participants with healthy lung and cardiac function were studied to determine the changes in shunting induced by 30 minute exposures to four levels of hypoxia: Fraction of Inspired Oxygen (FIO_2)=0.16, 0.14, 0.12, and 0.10. It was found that the threshold of hypoxic exposure to induce IPAV shunting in all subjects occurs at an FIO_2 of 0.10. It was also observed that shunt magnitude increased over the 30 minute exposure and with more severe levels of hypoxia and a limitation with the current shunt assessment methodology was identified. The development of a quantitative scoring system, using image analysis Adobe Photoshop software was then developed, which revealed trends in the data not previously noted due to limitations of the previous qualitative system used to assign shunt magnitude scores. Specifically, an inverse relationship between arterial oxygen tension and shunt magnitude was identified using this quantitative system. The

significance of these shunt pathways may be extensive as they could contribute to pulmonary gas exchange inefficiency and they may allow for emboli to bypass the pulmonary circulation resulting in neurological sequelae such as transient ischemic attacks, migraines and strokes.

Acknowledgements

The author would like to thank Professor Andrew Lovering and Steve Laurie for their exceptional support and guidance throughout the completion of this project. In addition, thanks are due to the rest of the Lovering Lab members: Ximeng Yang, Jon Elliott, Caitlyn Gust, Milind Nigam, Collin Bailey, Matt Hadeed, and Nick Colin for their participation in and contribution to this project. Special thanks also to Randy Goodman (Registered Diagnostic Cardiac Sonographer) his work on the project and insight into echocardiography.

Table of Contents:

Table of Figures:

Introduction:

Previous studies have demonstrated that intrapulmonary arteriovenous shunting is induced by exercise in normoxia and hypoxia in the majority of individuals as well as at rest in hypoxia in some individuals (8). In addition, a decrease in gas exchange as demonstrated by a widening of the $AaDO_2$, can be caused by an increase in shunting. Physiological factors that regulate the recruitment of these pathways have been postulated by authors of previous studies (10), but the exact mechanism remains unknown. This could partially be due to the observed individual variability in response to incremental exercise and hypoxia in terms of shunt pathway recruitment (3).

The original purpose of my study was to determine how IPAV shunt pathways respond to various levels of acute hypoxic exposure. We specifically wanted to know how the response would change over time and if there was a physiologic threshold level of hypoxia that could induce shunting in all subjects at rest. It was found that the mean shunt scores obtained with hypoxic exposure of fraction of inspired oxygen (FIO_2) 0.10 and 0.12, representing moderate and severe levels of hypoxia respectively, were qualitatively higher at 30 minutes of exposure than at 5 minutes of exposure (4). In addition, it was determined that an FIO2 of 0.10 resulted in a shunt score of more than 2 (which is the qualitative requirement for left sided contrast to be considered a shunt) at rest (3). At exposures of lower FIO2s=0.10 and 0.12, a plateau in qualitative shunt socre was observed over the 30 minute time span, although the qualitative magnitude of shunting actually continued to increase. However, due to the limitations of the current scoring system (0-5) this trend was not observed. In addition, when evaluating the bubble data we noted that it was often subjectively difficult to determine the difference between a shunt score of 4 and a score of 5 when assigning a score. It was also noted that

variability between images that were assigned the same shunt scores in the range of 3-5 indicated potentially significant differences in the magnitude of shunting, reflecting the insensitivity of the current (0-5) scoring system.

This prompted the development of a quantitative, less subjective, and more sensitive scoring system using image analysis software (Adobe Photoshop CS4), which became the primary focus of my work. The previous qualitative scoring system relied on the Registered Diagnostic Cardiac Sonographer assigning scores of 0-5 to varying degrees of left sided contrast detected based on previously set qualifications. The qualitative definitions of the scoring system developed by Lovering *et al*., *J Physiol* 2008, are based on both the amount and spatial distribution of bubbles in the left ventricle: a score of 0 represents a cloud of bubbles in the right heart, but no contrast in the left ventricle, 1 represents 1-3 bubbles in the left ventricle, 2 represents 4-12 bubbles in the left ventricle, 3 represents more than 12 bubbles in the form of a bolus in the left ventricle, 4 represents more than 12 bubbles that fill the left ventricle heterogeneously, and 5 represents homogeneous filling of the left ventricle (9). Although scores of 1 and 2 are quantitative, shunting is defined as achieving a shunt score of 2 or more (9). Therefore, this leaves only four out of six scores (one of which is quantitative) to represent all levels of physiologic shunting, which limits the sensitivity of the scoring system to reveal small changes in shunt magnitude. Additionally, because this system involves subjective descriptive analysis and assigning each image a score, the difference in the degree of shunting between scores is not equal or linear. A quantitative method was thus developed, employing a linear 0-20 scoring scale in order to assess the magnitude of shunting with greater objectivity and sensitivity. It was hypothesized that this will expand the shunt scores detected at lower levels of

hypoxia and may more accurately match the magnitude of shunting to changes in physiological variables such as arterial PO_2 (PaO_2), PASP, CO, etc.

Background:

Cardiopulmonary physiology and pulmonary gas exchange

The basic physiological function of pulmonary respiration is to allow the exchange of gases, mainly oxygen (O_2) and carbon dioxide (CO_2), between the body and the environment. Blood flows through the cardiopulmonary system as follows: systemic veins carrying deoxygenated blood from the body converge into the inferior and superior vena cava, which empty into the right atrium of the heart. Blood is then pumped to the right ventricle of the heart, which subsequently pumps deoxygenated blood to the pulmonary trunk. The pulmonary trunk splits into two pulmonary arteries, one going to each lung (18). Once inside the lung, blood flows through the pulmonary capillary beds, where it is oxygenated via gas exchange with air sacs inside the lung called alveoli. The blood then enters the pulmonary veins, returning it to the left atrium of the heart, which subsequently delivers blood to the left ventricle. When the left ventricle contracts blood is pumped to the aorta and dispersed to the rest of the body.

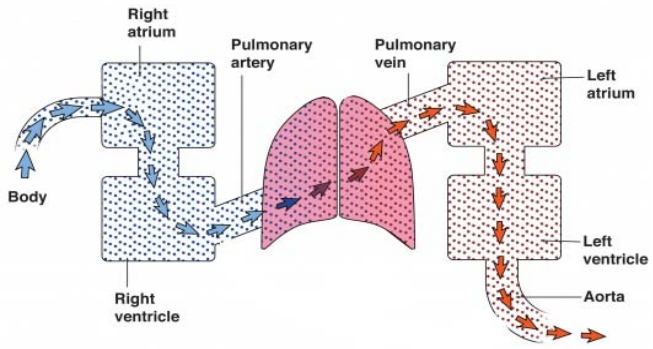

Figure 1. Blood flow through the cardiopulmonary system.

Gas exchange within the lungs includes the diffusion of O_2 into the blood and CO_2 out of the blood. Carbon dioxide is a waste product of metabolically active cells that use $O_2$to produce

energy. Blood circulation to the body delivers O_2 for consumption and removes CO_2. The exchange of gases both systemically and in the lungs is driven by the difference in concentrations (partial pressures) of gases in the blood and gases in the lung or body tissues, otherwise known as concentration gradients. Oxygen is carried in the blood by hemoglobin, a protein that regulates the uptake and release of oxygen under different chemical and physical constraints, as well as a dissolved gas. CO_2 is transported in the blood in three different ways: dissolved as CO_2, bound to hemoglobin, or in the form of bicarbonate (14).

Pulmonary gas exchange efficiency

In healthy individuals at rest, pulmonary gas exchange is considered relatively efficient. However, gas exchange becomes less efficient as the body's demand for oxygen increases, such as during high intensity exercise. There are four variables that can potentially contribute to the decrease in gas exchange efficiency. These variables include ventilation to perfusion nonuniformity gas diffusion limitations within the lungs; extrapulmonary shunt; and intrapulmonary shunt. If pulmonary gas exchange were perfect, the diffusion of oxygen from alveoli into the blood would be perfect and there would be no difference in the alveolar partial pressure of O_2 (PO_2) and the arterial PO_2. Inefficient gas exchange leads to an increase in the alveolar-to-arterial PO_2 difference ($AaDO_2$). This means that the difference between alveolar PO_2 and the PO_2 in arterial blood increases as gas exchange efficiency decreases (Fig. 2) (8).

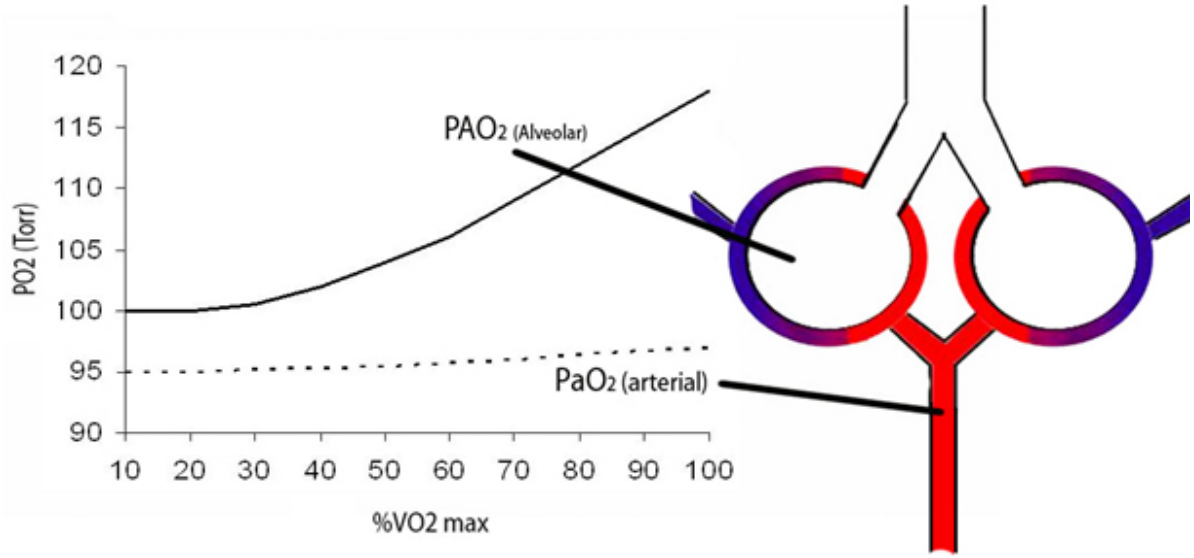

Figure 2 (3). Increased AaDO2 during exercise defines decreases in gas exchange efficiency.

Ventilation to perfusion matching, the first factor contributing to gas exchange efficiency, refers to the ratio of the volume of air ventilating the alveoli to the volume of blood being pumped through the pulmonary capillaries (perfusion). This is otherwise known as the V_A /Q ratio, where V_A refers to alveolar ventilation and Q refers to cardiac output (CO). Cardiac output is the amount of blood that the heart pumps per minute. In order for efficient gas exchange to occur the V_A/Q ratio needs to be close to 1.0 (14). In general, when pulmonary perfusion increases, such as during exercise, there is an equal or greater increase in alveolar ventilation. Thus, ventilation to perfusion matching maintains proper oxygenation of and CO_2 removal from the blood (14).

Diffusion, the second variable affecting gas exchange efficiency, is determined by four variables that can affect the ability of oxygen and carbon dioxide to diffuse between the pulmonary capillaries and the alveoli. These factors include the surface area for diffusion,

distance for diffusion, concentration gradient (partial pressures) of the gases, and the transit time of blood through the pulmonary capillaries. The surface area of diffusion is maximized by the alveoli and capillaries. The trachea branches into two primary bronchi, which further branch into secondary bronchi, and then again into bronchioles, which turn into alveolar sacs each of which contain individual alveoli that have very thin walls, allowing for efficient gas diffusion into and out of them (18). The total surface area of all alveoli together equals roughly the size of a tennis court (14). Blood exchanges gases with alveolar air through capillary walls. Capillaries are fed by arterioles (small arteries), which are fed by arteries. The walls of capillary vessels are made up of a very thin, single layer of epithelial cells, which are permeable to gases. The extensive branching of airways and blood vessels allow the surface area of diffusion between capillaries and alveoli to be maximized, while simultaneously the distance for the diffusion of gases is minimized.

These two physical factors allow for the efficient diffusion of gases, but the driving force of gas exchange is the concentration gradients of O_2 and CO_2 in the pulmonary capillary and the alveolus. The partial pressure of an individual gas in air is equal to the product of the total pressure of the air (barometric pressure) and the fractional component of that particular gas. For example, the partial pressure of oxygen at sea level is: PO_2= 760 mm Hg (absolute barometric pressure) X 0.2093 (fractional component of oxygen in the air). So partial pressure of an inspired gas at sea level would be 760 – 47 Torr (water vapor pressure) x 0.2093. The partial pressure of oxygen and carbon dioxide in alveolar gases are 105 mm Hg and 40 mm Hg, respectively. In deoxygenated blood entering the lung they are 40 mm Hg for oxygen and 46 mm Hg for carbon dioxide. Gases diffuse from areas of high concentration to areas of low

concentration, meaning that oxygen will move into the blood and carbon dioxide will move out of the blood in the lungs. This results in blood leaving the lung with a PO_2 of 100 mm Hg and a PCO_2 of 40 mm Hg.

The ability of the blood to properly exchange gases is also dependent on the amount of time that the blood takes to travel through the capillaries, and thus the amount of time it has to equilibrate with the alveolar air. This is referred to as transit time, which is regulated mainly by cardiac output and decreases with exercise as the velocity of blood being pumped through the pulmonary circulation increases. The average transit time is about 750 ms, and at maximal exercise this can drop to 450 ms (2). The amount of time it takes for gases completely equilibrate across the capillary-alveolar interface is dependent upon the oxygen tension in the air, which determines the driving force of oxygen into the deoxygenated blood. At low levels of oxygen tension, such as at altitude, the time it takes to fully equilibrate gases increases, and thus maximal transit time during exercise may not allow for full oxygenation of blood, leading to arterial desaturation. However, at sea level, transit time is more than sufficient for complete gas exchange to occur.

Another component that can contribute to gas exchange inefficiency is non-pulmonary shunting, which is defined as shunt pathways that deliver deoxygenated blood directly to the left atrium without passing through the lungs (19). There are three main types of non-pulmonary shunt pathways including intracardiac, and bronchial and thebesian venous drainage. Intracardiac shunting occurs through the patent foramen ovale (PFO), which is a structure in the heart that allows for blood to pass between the right and left atrium in a fetus, as only 10% of

the cardiac output passes through the lungs during development (12). This shunt pathway does not completely close in all adults (~30%), which results in small amounts deoxygenated blood from the right atrium passing directly to the left ventricle without being pumped through the lungs. However, this is only possible if right atrial pressure exceed left atrial pressure. Thus, during rest PFO can contribute to the widening of the $AaDO_2$, however it does not during exercise (Lovering AT, Stickland MK, Amann M, Carlson JM, Hokanson JS, and Eldridge MW. *Experimental Biology*. Poster, 2008). Bronchial circulation and thebesian circulation shunts return blood directly to the left atrium of the heart via bronchial and thebesian veins. Therefore, they bypass pulmonary circulation, and decrease the PO_2 of blood pumped to the rest of the body (19).

The last factor that contributes to $AaDO_2$ widening is intrapulmonary shunting, which is the main focus of my thesis. Intrapulmonary shunts are defined as blood that enters pulmonary circulation but bypasses the pulmonary capillary beds and therefore does not participate in pulmonary gas exchange (2). Deoxygenated blood is returned to the heart to be pumped to the rest of the body along with oxygenated blood that did participate in gas exchange in the lungs. This partially deoxygenated blood becomes progressively deoxygenated as working muscles continually extract oxygen. Therefore, the amount of blood that travels through intrapulmonary shunt pathways does not need to be very large (about 1-3% of Q) in order for a significant change in $AaDO_2$ to result (2). Previously, the widening of $AaDO_2$ during exercise has been attributed mostly to V_A/Q mismatching. However, not all individuals exhibit V_A/Q mismatch during exercise, but all subjects show a widening of $AaDO_2$ (2). In addition, Stickland, et al. discovered that an $AaDO_2$ of 12 Torr or more was always associated with intrapulmonary

arteriovenous shunting (19). These data strongly suggest an important role of IPAV shunts in gas exchange.

It is well known that $AaDO_2$ widens during high intensity exercise. During maximal exercise it has been determined that $AaDO_2$ reaches values of 20-30 Torr in healthy, untrained subjects. In elite athletes this may reach values up to 35-50 Torr (2) because the physical size of an individual's lungs becomes the limiting factor to pulmonary gas exchange. An important note to make regarding $AaDO_2$ widening in relation to exercise is that it is mainly determined by intensity, or metabolic rate, not duration. One study found that subjects working at a constant high intensity saw no changes in gas exchange efficiency over time, but with progressive, submaximal exercise, a direct correlation of increases in $AaDO_2$ with increases in workload was observed (19). Decreasing pulmonary gas exchange efficiency during exercise leads to exercise induced hypoxemia, which is characterized by a decrease in hemoglobin saturation (SaO_2) of the arterial blood and results in a decrease in exercise capacity at a given workload (6). Consequently, this decrease in SaO_2 leads to fatigue and reduced exercise performance.

Anatomic evidence of shunt pathways

Large diameter intrapulmonary arteriovenous (IPAV) shunt pathways provide a non-capillary passage for blood to bypass the alveoli and will therefore contribute to a decrease in gas exchange efficiency. These have been identified in a wide range of species (11), (20) using a variety of methods. Tobin *et al.* provided evidence for the existence and size of these pathways by studying plastic casts of human lungs and demonstrating that glass or resin beads of 50-200 μm in diameter could bypass the pulmonary capillaries (21), (22). The passage of micro bubbles

across the pulmonary vasculature in exercising humans was described by Eldridge *et al.* in 2004 and it was estimated that the micro bubbles were 60-90 μm in diameter based on the survival time of bubbles suspended in blood (2). Stickland *et al.* detected the passage of 25 μm polymer microspheres in exercising dog (20), while 50 μm mircoshperes were found to bypass isolated and perfused human and baboon lungs (11). The passage of blood through inducible pathways would contribute to inefficient gas exchange in the lungs due to limited gas exchange through the thick vessel walls, estimated to be ~2.5 μm thick; whereas, capillary wall thickness, which is ideal for gas exchange, is only ~0.2 μm thick (19). Although the exact identity of these IPAV vessels is unknown, IPAV shunts have been demonstrated in fetal lungs of both humans and lambs and in lambs have been shown to become inactive postnatally (13). Accordingly, these remnant fetal vessels may possibly be the origin of IPAV shunts that are recruited during exercise and hypoxia adults (8).

Physical characteristics of saline contrast bubbles

Saline contrast bubbles that are injected into a peripheral vein are subsequently either trapped in the pulmonary vasculature or bypass it and end up on the arterial side of the circulation. Because polymer microspheres cannot be used in healthy human subjects, we utilize a technique using saline contrast micro bubbles. The exact size and number of saline contrast bubbles cannot be determined. Therefore, it is necessary to consider "basic" physics of bubbles in order to estimate the size of bubbles that are seen in the left ventricle with saline contrast echocardiography. The factors that will contribute to this include survival time of the bubble in the blood, blood flow rate, and vascular pressure. It is very unlikely that microbubbles are

passing through pulmonary capillaries (7-10 um in diameter) as bubbles of this size have a survival time of only 190-550 ms in static fluid (10) and it takes at least 1 second for blood to pass from the right heart to the left heart a heart rate of 180 bpm (typically achieved only during maximal exercise). During exercise blood flow and pressure would also be increased, resulting in a further reduction in survival time of these bubbles (8). Additionally, if these bubbles could squeeze through capillaries, we would see their accumulation in the left heart in all subjects during every injection, yet we do not. Similar blood flow and pressure changes occur in hypoxia, another condition that has been identified to recruit these passages (3).

Recruitment of IPAV shunts during exercise and in hypoxia

Saline contrast echocardiography has detected the recruitment of IPAV shunt pathways to increase with exercise intensity in 90% of healthy humans (2). This observed recruitment trend led authors to postulate that the vessels are opened with elevated pulmonary vascular pressure and blood flow velocities. Lovering et al. determined that hypoxia augments IPAV shunt recruitment during exercise and opened these pathways in 3/9 subjects at rest, which supports a proposed mechanism governing the patency of the shunt vessels to acute hypoxic exposure leading to increased pulmonary vascular pressure as a result of hypoxic pulmonary vasoconstriction and cardiac output (8). It was also determined from this study that at the same submaximal levels of exercise the degree of shunting was greater in hypoxia than in normoxia. The findings from this study provide evidence for the possible importance of IPAV shunts in providing a parallel vascular network for blood flow to bypass the pulmonary resistance vessels and minimize increases in pulmonary artery pressure, which could damage pulmonary capillaries or lead to pulmonary edema (8). Although the majority of subjects showed increased

shunt recruitment in hypoxia at rest, some individuals did not respond to the lower oxygen tension (8). The reasons for individual variability in the conditions under which shunt pathways are recruited in hypoxia remain unknown.

Limitations with the use of saline contrast echocardiography to detect intrapulmonary arteriovenous shunting

Although the use of contrast echocardiography is well established, having been used as early as 1976 by Shub et al (17), one limitation is the inability to quantify the saline contrast detected in the left ventricle. A major advance in echocardiography was the development of second harmonic imaging, which optimizes both penetration and spatial resolution of the image (16). This enhances the signal-to-noise ratio, thereby improving the ability to see contrast bubbles in the left ventricle (8). However, currently*, only qualitative measures exist to indicate the degree of shunting*. Previously, this has been less of a problem as qualitative scores were sufficient to conclude an increase in shunt intensity with exercise intensity or the presence of shunting at rest in hypoxia. However, now that intrapulmonary arteriovenous shunting is known to occur in these situations, attempting to tease out the mechanisms that regulate these pathways requires a more sensitive scoring system to elucidate the trends in physiological measurements that occur in relation to the degree and progression of shunting. Thus, the goal of my project was to develop a more sensitive, objective technique for measuring left heart saline contrast.

Methods:

Approval for this study was obtained from the University of Oregon Institutional Review Board and informed consent forms were signed by all subjects. All studies were performed according to the Declaration of Helsinki.

Subjects

Fifteen healthy subjects (six female) between the ages of 18 and 40 volunteered to participate in this study. A cardiopulmonary history was taken prior to participation and an echocardiographic screening was performed to eliminate subjects who dispayed the presence of a PFO or an arteriovenous malformation as these would display contrast in the left ventricle without IPAV shunting and contribute to inefficient gas exchange (8). A positive PFO was defined as the presence of contrast bubbles appearing in the left ventricle in less than three heart beats (8). Subjects with a PFO were excluded from the study as intracardiac shunting can contribute to gas exchange inefficiency (7).

Pulmonary function and lung diffusion capacity for carbon monoxide testing

Preliminary tests performed include pulmonary function tests, whole body plethysmography, and diffusion capacity of carbon monoxide to ensure normal healthy lung function (7), to measure lung function, lung volume, and diffusion capacity of the lung.

Resting hypoxia protocol

On the second study day, subjects rested in a reclined position and rolled 45˚ onto their left side in order to obtain a 4-chamber apical view of the heart. They breathed four levels of

hypoxia with fractions of inspired oxygen (FIO_2) of 0.16, 0.14, 0.12, and 0.10. These gases containing different oxygen tensions were breathed in either an increasing or decreasing order (7). Before each acute hypoxic exposure the subject breathed normoxic (room) air, with an FIO_2 of 0.21, for five minutes. This was followed by thirty minutes of breathing hypoxic air. Saline contrast bubbles were injected and an echocardiogram was simultaneously recorded at four minutes into normoxia (right before beginning exposure to hypoxia) and then every five minutes following the onset of hypoxic exposure. After each hypoxic exposure subjects were given a 15 minute break breathing room air.

Contrast echocardiography and the 0-5 scoring system

The presence of IPAV shunting is detected using saline contrast echocardiography, which consists of manually agitating 3 mL of sterile saline with 1 mL of air, and forcefully injecting the saline contrast into a peripheral vein in the arm through an intravenous catheter while simultaneously imaging the heart using ultrasound (echocardiogram). Shunting occurs when the microbubbles, seen as echoes in the image, appear in the left ventricle of the heart three cardiac cycles following the appearance of contrast bubbles in the right ventricle (8). If there is no shunt, all micro bubbles will be filtered out by the pulmonary capillaries. The presence of contrast bubbles in the left ventricle indicates that microbubbles were able to traverse the pulmonary circulation and pass into the pulmonary vein via patent IPAV shunt pathways (2). Because this does not occur during rest, we know these bubbles do not traverse through capillaries. The magnitude of a detected shunt is qualitatively assigned using the 0-5 numbering system discussed above (9). However, the exact size of the bubbles that reach the left ventricle is unknown (19).

Image analysis and the 0-20 scoring system

All images were obtained from the echocardiogram recordings and analyzed in Adobe Photoshop CS4 software. Images were selected from frames previewed in Photoshop by scrolling through the series of images for each (~30 frames/second) cardiac cycles in each recording and visually determining the range of cardiac cycles in which the highest degree of shunting was detected. From one of the cardiac cycles showing peak bubble density, the three individual frames with the most visible bubble contrast were selected for image analysis. However, if the magnitude of shunting was small enough that it was possible to count individual isolated bubbles in the left ventricle, only the frame with the most bubbles was selected. In addition, image analysis was not subsequently performed on these images due to limitations and errors introduced by contrast of the left ventricle wall in the same area of interest as the contrast microbubbles. Instead, the number of bubbles counted in the selected frame was multiplied by the average size of one bubble, which was found to be 15 pixels, and a score assigned based on the resulting value (scoring system described below).

The main goal of the processing of these images in Photoshop was to produce an image in which the relative features were adequately separated from the background, called segmenting, so that areas of interest could be automatically selected. Although the segmenting methods enabled by Photoshop are superior to other image analysis programs, they cannot "provide absolutely exact measurements: Rather, the methods provide a consistent means for obtaining statistically accurate results when derived from a number of measured images"(15).

The images in this study were processed using a combination of two actions, each of which included a series of preset image manipulations. The first action includes the use of a gradient map applied twice, once to the original image and then applied again on top of that image (Fig. 3.2). The gradient map allows certain tones of gray to be mapped to gray. The result is a sharper image with less "noise" and better defined bubble edges. After the first action was played in Photoshop, the magnetic lasso tool was used to select the inside of the left ventricle (Fig. 3.3). The settings used for the magnetic lasso tool are as follows: feather=0px, width=3px, contrast=70%, and frequency=68. These preset values provided optimal sensitivity for selection around the inside of the left ventricle wall. If the mitral valve (between the left atrium and left ventricle) was included in the selection and could easily be seen separately from bubbles the paint brush tool was used to paint over these areas with black in order to exclude these artifacts from the white contrast seen in the left ventricle. The second action was then played, which started with transformation of the previous selection to 90% of its size in both height and width (Fig. 3.4) to eliminate any white contrast from the ventricle wall that may still be inside the original selection. This selection was then inverted, resulting in selection of the entire image around the left ventricle, allowing this area to be deleted from the images, which enabled subsequent automatic selection of only features within the left ventricle. Before selection, a high pass filter was applied to the remaining pixels (Fig. 3.5), which further sharpens the image(15). The highlights that remained in the image were then automatically selected using the following set of commands in Photoshop: Select→ Color Range→ Highlights (Fig. 3.6). The total area of this selection was then recorded in terms of the number of pixels using the measurement log.

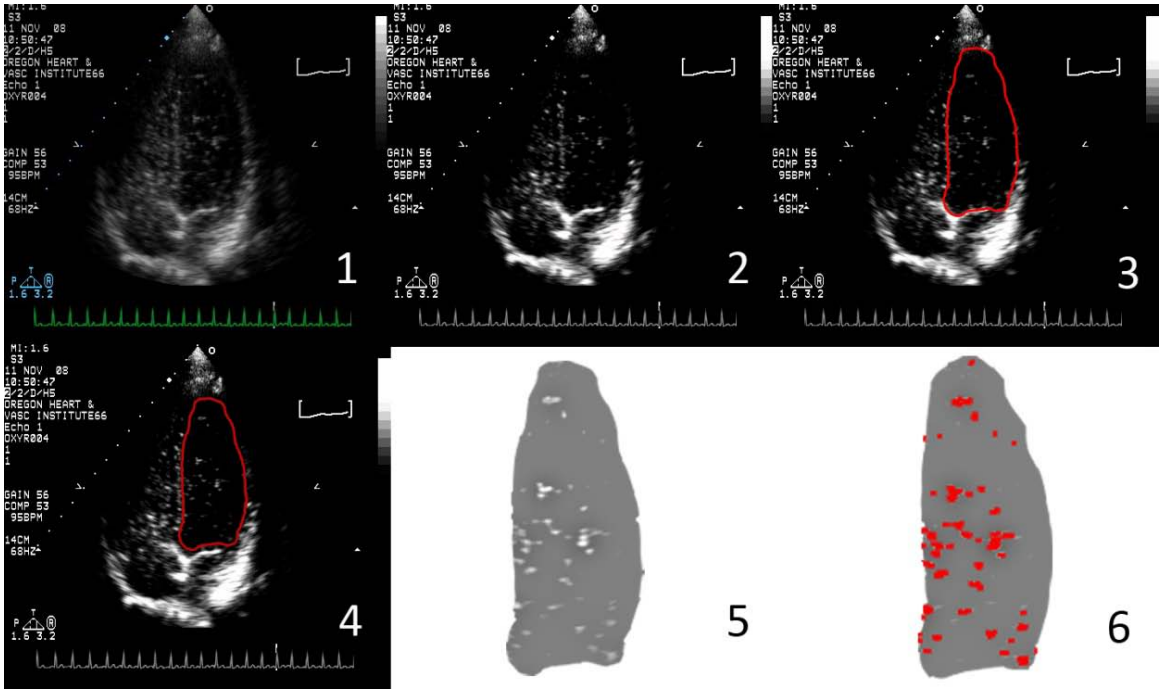

Figure 3. Steps of in image analysis and segmentation procedure to obtain 0-20 shunt scores.

This series of actions was performed on all three frames of the cardiac cycle that were previously selected. The measurements obtained were put into excel, averaged and assigned a score of 2-20 based on the resulting average area of bubbles selected in the three peak contrast frames. In the 0-20 scoring system each value represents a range of 100 pixels. An area range of 1-100 pixels was assigned a score of 1, the range 101-200 a score of 2, and so forth. This method of bubble selection and quantification provides an objective score that eliminates the biases associated with image interpretation and assignment of qualitative scores. Additionally, the resulting scoring system is a linear quantification such that the difference in the degree of shunting between scores is uniform.

Results:

Timing effect on magnitude of shunt over time

Using the 0-5 scoring system, it was found that as the FIO_2 decreased, and thus the severity of hypoxia increased, higher shunt scores were achieved. The mean shunt score for each FIO_2 at 30 minutes was 0.75 at FIO_2=0.16, 1.5 at FIO_2=0.14, 2.17 at FIO_2=0.12, and 3.33 at FIO_2=0.10 (Fig. 4). In addition, the magnitude of shunting increased throughout the 30 minute exposure. The increase in average shunt score from 5 to 30 minutes of hypoxic exposure was 1.0 at FIO_2=0.10, 1.25 at FIO_2=0.12, 0.58 at FIO_2=0.14, and 0.25 at FIO_2=0.10. These differences show an increasing change in shunt score with more severe levels of hypoxia with the exception of the increase seen at FIO_2=0.10, which is 0.25 less than the increase seen at FIO_2=0.12. Furthermore, there was a significant plateau in shunt magnitude over time at an FIO_2 of 0.10, and at an FIO_2 of 0.12. However, at FIO_2 of 0.14 and 0.16, where the degree of hypoxia was not as severe, the average shunt score was less than two for the entire duration and the plateau observed at lower FIO_2 levels was not observed.

Using the 0-20 scoring system it was seen that as the FIO_2 level decreased the average shunt scores increased with the average of each hypoxic level at 30 minutes being 16 at FIO_2=0.10, 7 at FIO_2=0.12, 3 at FIO_2=0.14, and 1.5 at FIO_2=0.16 (Fig. 5). In addition, it is seen that the magnitude of shunting increases with time over the 30 minute exposure. The increase in average shunt score achieved between 5 and 30 minutes of hypoxic exposure was 9.5 at FIO_2=0.10, 5 at FIO_2=0.12, 2 at FIO_2=0.14, and 0.5 at FIO_2=0.10. These differences show an increasing change in shunt score with more severe levels of hypoxia for all levels of hypoxic

exposure, which was not seen with the 0-5 scoring system. Furthermore, the steep increase in shunt magnitude followed by a prolonged plateau at lower FIO_2 levels is not observed using the 0-20 scale. In addition, at FIO_2 of 0.14 and 0.16, where the degree of hypoxia was not as severe, the slopes of the curves are relatively flat compared to the slopes achieved at FIO_2 of 0.10 and 0.12.

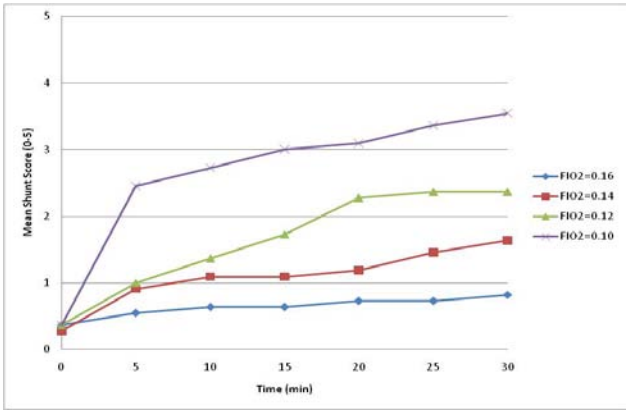

Figure 4. Average shunt score achieved over 30 minutes at various levels of hypoxic exposure using the 0-5 scoring system. Average shunt scores of11 subjects using the 0-5 scale breathing 4 levels of hypoxia for 30 minutes at rest.

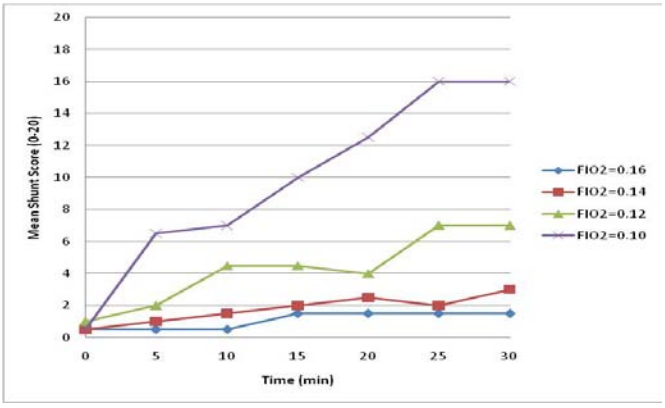

Figure 5. Average shunt score achieved over 30 minutes at various levels of hypoxic exposure using the 0-20 scoring system. Analysis of shunt scores for 2 subjects using the 0-20 scale breathing four levels of hypoxia for 30 minutes at rest. Note the greater difference in shunt score from FIO_2=0.12 to FIO_2=0.10 as compared with the 0-5 scale in Fig. 4.

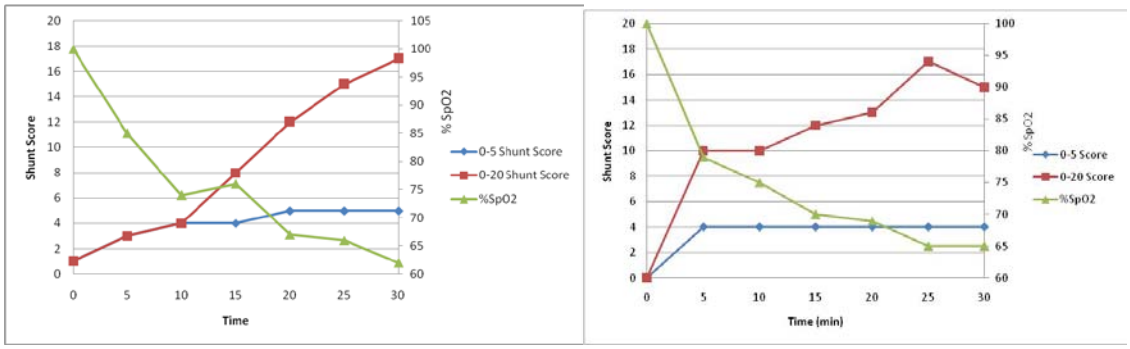

Figure 6. a) Subject #1 at FIO2=0.10. b) Subject #2 at FIO_2=0.10.

Using the 0-20 scale a better inverse relationship was observed between shunt score and SpO_2 than was seen using the 0-5 scoring system (Fig. 6). Figures 6a and 6b show the SpO_2 and the average shunt scores, using both the 0-5 and 0-20 shunt score scales, of two individual subjects achieved over the 30 minute hypoxic exposure. In Fig. 6a the shunt magnitude plateaus at 20 minutes of exposure while achieving the highest possible shunt score of 5 for the remainder of the hypoxic stage. Using the 0-20 scale, the magnitude of shunting continues to increase over the entire 30 minutes of exposure without a significant decrease in slope at later time points. In addition, the SpO_2 of this subject at FIO_2=0.10 continues to decrease across the 30 minute exposure. Fig. 6b shows similar results for subject #2 at the same FIO_2, in that using the 0-5 scale the subject plateaus at a score of 4 after only five minutes of exposure, whereas using the 0-20 scale no plateau is observed. This individual also shows a similar SpO_2 trend that continues to decrease across the 30 minutes of exposure and is inversely proportional to shunt score magnitude.

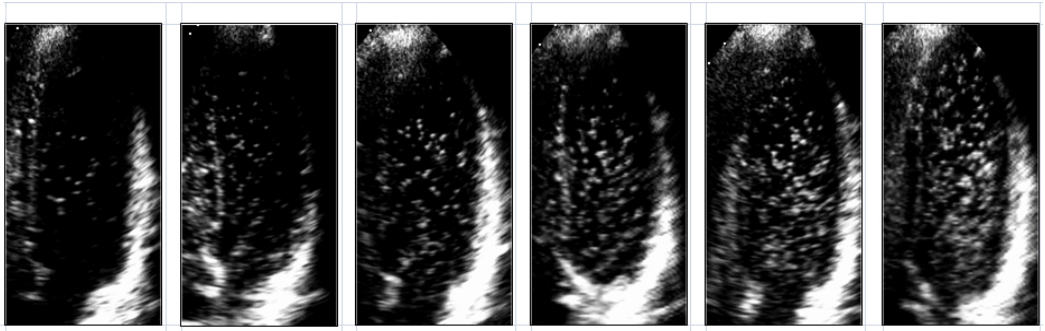

Time (min)	5	10	15	20	25	30
Area (px)	231	380	830	976	1464	1544
0-20 Score	**3**	**4**	**9**	**10**	**15**	**16**
0-5 Score	**3**	**4**	**4**	**5**	**5**	**5**

Figure 7. Quantitative vs. qualitative differences in shunt scores.

Figure 7 illustrates the shunt scores presented in Fig. 6a starting with 5 minutes of hypoxic exposure. The row showing the area indicates the number of white pixels selected in Photoshop, which represents the amount of area covered by bubbles. The area selected in each frame continues to increase with increasing duration of hypoxic exposure. It was observed that images obtained at 15, 20, and 25 minutes appeared similar and had the same or very similar shunt scores using the 0-5 score, but the area of bubbles in each is calculated to be significantly different, and were different using the 0-20 score.

Identification of the threshold for hypoxia-induced IPAV shunting in humans at rest

Figure 8a shows the average shunt score (11 subjects) achieved at each given FIO_2 as well as the corresponding $\%SpO_2$. The red line indicates the threshold level of hypoxic exposure that was able to induce IPAV shunting in all subjects, defined as achieving a shunt score of 2 or greater using the 0-5 scoring system, was achieved at an FIO_2 of 0.10. In addition, it is seen that shunting is also induced in the later stages (20, 25, and 30 minutes) of hypoxic exposure to an

FIO_2 of 0.12 in the majority of subjects. Figure 8b also shows the average shunt score (2 subjects) achieved at each FIO_2 and the corresponding $\%SpO_2$. In addition, the red line indicates that the threshold for hypoxia-induced shunting is still achieved at an FIO_2=0.10 when the 0-20 shunt scoring system is used.

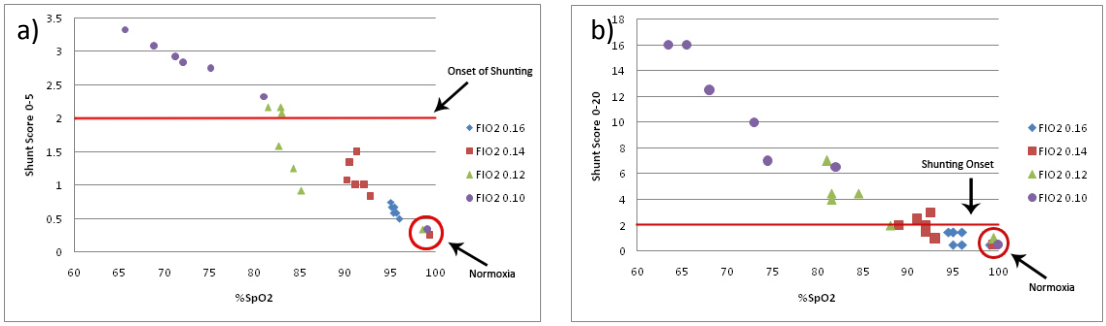

Figure 8. Threshold for hypoxia-induced shunting a) using the 0-5 scoring system and b) using the 0-20 scoring system.

Discussion:

The purpose of this study was twofold. First we sought to determine how the recruitment of intrapulmonary arteriovenous shunt pathways changes over time and at varying levels of hypoxic oxygen tensions in attempt to elucidate the physiological conditions that contribute to their regulation. Breathing hypoxic gas caused an increase in shunting intensity over thirty minutes at all hypoxic levels tested (FIO_2=0.16, 0.14, 0.12, and 0.10) whether subjects breathed gases in an ascending or descending order. Additionally, average shunt score (*n*=11) increased with more severe levels of hypoxia at any given time point from 5-30 minutes following the onset of hypoxic exposure. Although some individuals responded more than

others (i.e. shunting increased more or less intense) to given levels of hypoxic exposure, when exposed to an FIO_2 of 0.10 shunting was induced in all subjects, making this level of hypoxic exposure the threshold that will induce shunting at rest in all individuals. An inverse relationship between shunt score intensity and SpO_2 was observed, but at the lower FIO_2 levels of 0.12 and 0.10 SpO_2 continued to decrease across the thirty minutes of exposure (Fig. 9) while shunt score plateaus at the higher intensities of shunting (Fig. 4).

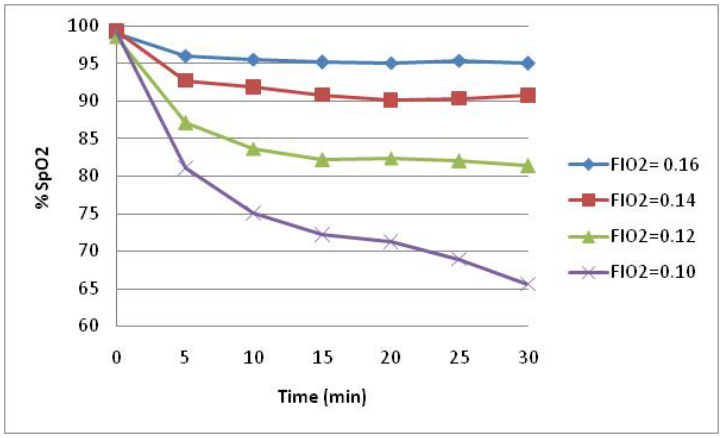

Figure 9. %SpO_2 vs. time. This graph shows the % SpO_2 achieved over time at each level of hypoxic exposure. % SpO_2 continued to decrease throughout the duration of hypoxic exposure at FIO_2s of 0.10 and 0.12, while % SpO_2 values at FIO_2s of 0.14 and 0.16 show a significant plateau in shunt magnitude across the duration of hypoxic exposure.

Second, a new scoring system was developed in response to the observation that SpO_2 continually dropped across the 30 minutes of hypoxic exposure while shunt magnitude reached a plateau. As oxygen tension plays a key role in the regulation of these shunt pathways, shunt magnitude would be expected to mirror SpO_2. The 0-20 scoring system developed using Adobe Photoshop CS4 software enabled the quantification of intrapulmonary arteriovenous shunting and revealed significant differences in individual shunting events that previously received the same qualitative score of 0-5. The main difference between the shunt scoring systems exists at

higher levels of shunting, which includes events previously qualitatively scored as 3, 4, or 5. Shunt score bubble intensity continually increased throughout the duration of hypoxic exposure when the new quantitative shunt scoring system with a scale of 0-20 was employed to assign shunt scores. In addition, as shunt score increased across the 30 minute hypoxic exposure using the new scoring system, a better matched inverse relationship between SpO_2 and shunt score was observed (Fig. 6). Although this further supports that oxygen tension plays a key regulatory role in the recruitment of these shunt pathways it is still unclear if this interaction directly affects characteristics of these shunt vessels or is indirect due the resulting effects of hypoxia on the rest of the pulmonary vasculature (i.e. non-shunt vessels) (8).

Shunting increases with increasing hypoxic exposure duration:

The increase in magnitude of shunt score achieved at longer exposures of hypoxia, and with increasing severity of hypoxia at all levels of FIO_2, combined with the concomitant decrease in SpO_2 over time, provides strong evidence that the recruitment of shunt pathways may be partially regulated, either directly or indirectly, by some oxygen sensor such as the peripheral chemoreceptors. Peripheral chemoreceptors monitor the PO_2 of the blood, and include two aortic and two carotid bodies that are located at the aorta and at the bifurcation of the common carotid artery respectively. When a change in PO_2 of the blood is sensed, peripheral chemoreceptors (mainly the carotid bodies) increase their firing rate resulting in an increased minute ventilation (volume of air breathed per minute). Due to the fact that saline contrast bubbles are observed to be more dense when lower SpO_2 values are reached, it is possible that this increase in shunting magnitude could be associated with increased activation of the peripheral chemoreceptors, thereby causing increased firing rate in an intensity dependent

manner (12). Although the trend of increased shunting intensity with lower SpO_2 values was observed in previous studies (8), (9) the development of the 0-20 scoring system, has allowed for a more detailed correlation to be observed between physiological variables such as pulmonary artery pressure, cardiac output, hypoxic ventilatory response, etc. This better resolution of correlations will allow us to better formulate future research ideas and hypotheses.

Determination of a threshold for hypoxia-induced intrapulmonary arteriovenous shunting

The highest level of hypoxic gas at which shunting was detected in all subjects was at an FIO_2 of 0.10. This represents severe hypoxic conditions as it is about half the normal content of oxygen in the air and corresponds to approximately 18,862 ft elevation. Despite this seemingly high threshold, many subjects began shunting at low and moderate levels of hypoxia. Two of 11 began shunting at an FIO_2 of 0.16, 5/11 started shunting at an FIO_2 of 0.14, and 1/11 started shunting at an FIO_2 of 0.12. The majority of subjects started shunting before an FIO_2 of 0.10, which indicates a wide range of sensitivity to hypoxia between individuals. When this trend was evaluated with the new 0-20 scoring system no significant changes were noted in the general distribution of shunt scores 1 and 2, and as shunt onset is defined as achieving a score of 2 or greater using the 0-5 scale, the level of hypoxia at which shunting was detected in all subjects remained the same. However, because the ventilatory response to hypoxia is highly variable between individuals, a more sensitive determination of shunt, such as the 0-20 scoring scale, will allow for a more adequate evaluation of the correlation between shunt score produced by each individual and that individual's hypoxic chemosensitivity.

Image analysis: qualitative vs. quantitative scoring system

Saline contrast echocardiography is a well-established method of studying intrapulmonary shunting both during exercise and in hypoxic conditions (2), (8), (9), (10). The detection of shunts with left sided contrast with an echocardiogram is critically important to the nature of this research. However, previous studies that employed the use of saline contrast echocardiography to detect left sided contrast and the presence of intrapulmonary shunting were mainly aimed at determining the physiological conditions, such as exercise and hypoxia, which initiate recruitment of shunt pathways, and/or qualitatively change the degree of shunting. Therefore, the necessity of a more sensitive scoring system was minimal (2), (10), (19), (9), (8). One purpose of this study was to systematically determine specific changes in shunting at various hypoxic exposures, and the results obtained with the 0-5 scale were not sufficiently sensitive to accurately distinguish differences in shunt magnitude at higher levels of shunting. The 0-20 quantitative scale was developed in attempt to remedy this. In Fig. 7 this can be seen in images from one frame to the next, representing a sequence of shunt scores across a 30 minute exposure, are difficult to distinguish between. However, when analyzed using Photoshop a significant difference in the amount of bubbles between very similar frames is detected. This is noticed most at shunt scores of 4 and 5 as is represented by Fig. 10, which shows the distribution of 0-20 shunt scores at each level of previously assigned scores of 0-5.

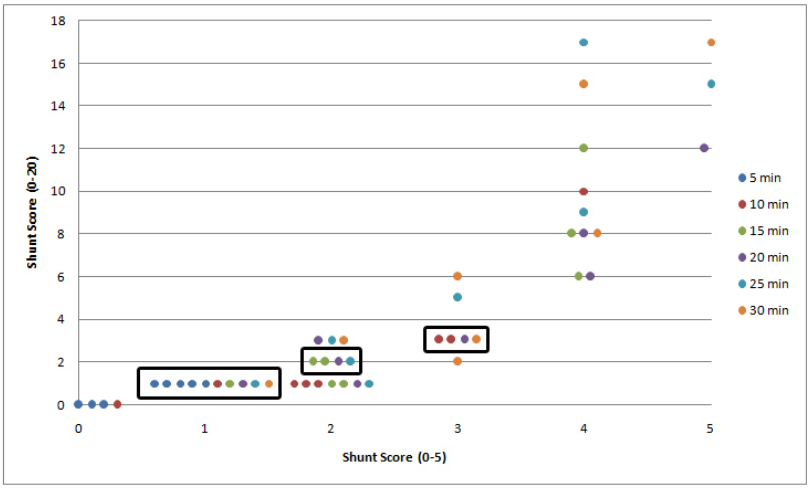

Figure 10. 0-5 shunts scores vs. 0-20 shunt scores. This graphs shows the individual 0-5 shunt scores achieved by subjects #1 and #2 at all FIO_2s and time points against the corresponding 0-20 shunt score assigned. The boxed points represent original shunt scores of 0-5 that did not change when 0-20 scores were assigned.

Difficulties developing 0-20 shunt score scale

Using image analysis and manipulation to obtain quantitative measures is becoming increasingly utilized in scientific research (15). However, there are parameters around which images can be manipulated to obtain quantitative information. The use of echocardiography to detect intrapulmonary shunting poses some possible difficulties to the quantification of shunt scores; these include a) the low resolution of images, b) significant amounts of background noise at low shunt scores due to detection of cardiac wall motion, and c) "apparent contrast" within the left ventricle caused by movement of the mitral valve throughout the cardiac cycle. Most of these problems were accounted for by combining the (0-20) method with the previous scoring system (0-5) of counting individual bubbles at very low shunt scores (0-1 on 0-5 scale), which generally consisted of between 1 and 15 bubbles. This was possible due to the sufficient

dispersion and isolation of contrast bubbles within the left ventricle as well as minimization of the background from wall motion and mitral valve "noise" was minimized at higher shunt scores simply because in most cases the bubbles were covering these areas that could have potentially confounded our attempts to quantify saline bubble contrast.

Conclusion:

From this study it was determined that the intensity of intrapulmonary arteriovenous shunt magnitude increased with time over a 30 minute acute hypoxic exposure and with increasing severity of hypoxia. In addition, a threshold at which shunting occurs in all subjects was determined to occur at an FIO_2=0.10. The development of a quantitative scoring system using a scale of 0-20, enhanced the variability seen between shunt scores that were previously assigned qualitative values of 0-5, using a previously determined qualitative scoring system (9). The quantitative system revealed a significantly closer inverse relationship between % SpO_2 and shunt score over time than was previously observed using the 0-5 scoring system. In addition, it showed that shunt magnitude did not plateau over 30 minutes at moderate and severe levels of hypoxia as was previously noted using the 0-5 scale. Furthermore, use of the 0-20 quantitative scoring system is expected to help identify other physiological factors governing the recruitment of IPAV shunt pathways that have yet to be determined.

Applications:

As intrapulmonary arteriovenous shunts are associated with gas exchange efficiency in the lung they should be considered in regard to ascent to high altitude where the barometric

pressure drops with increasing elevation, thus decreasing the alveolar oxygen tension, and therefore, the amount of oxygen that can diffuse into the pulmonary capillary blood. In response to hypoxia, the pulmonary vasculature vasoconstricts, resulting in increased pulmonary arterial pressure (PAP) (12). Individuals prone to developing high altitude pulmonary edema (HAPE) also have higher PAP values and increased pulmonary vascular resistance. This may indicate that these individuals to not have IPAV shunt pathways, which may act to mitigate the increase in PAP by decreasing the amount of blood flow that must pass through the pulmonary capillaries. In this case, the shunts would act as a protective mechanism to the delicate and thin walled pulmonary capillaries that can be damaged with high vascular pressures, which can be associated with the development of HAPE(2).

Furthermore, recent evidence from Loeppky *et al.* supports the concept of IPAV shunt pathway recruitment at high altitudes as they determined a relationship between the development of acute mountain sickness (AMS) and decreasing $SaO_{2\,(5)}$. This may indicate that individuals that have IPAV shunts and recruit them under low levels of hypoxia may be more susceptible to developing AMS at lower altitudes than subjects who do not recruit IPAV shunts and don't get AMS, as the presence of shunting has been shown to decrease arterial oxygen saturation. With ascent to high altitude there is also an increase in the prevalence of neurological insults such as transient ischemic attacks, strokes and migraines (1). This may be associated with the recruitment of IPAV shunt pathways in hypoxia that bypass the narrow pulmonary capillaries decrease the filtering ability of the lungs, thereby possibly allowing small blood clots and other emboli to travel through the lungs and adversely impact the brain.

Clearly, these inducible IPAV vessels have the potential to impact multiple physiologic and pathophysiologic processes in both health and disease states.

References:

1. **Basnyat B WT, Gertsch JH.** Neurological Conditions at Altitude That Fall Outside the Usual Definition of Altitude Sickness. *High Alt Med Biol* 5: 171-179, 2004.

2. **Eldridge MW, Dempsey JA, Haverkamp HC, Lovering AT, and Hokanson JS.** Exercise-induced intrapulmonary arteriovenous shunting in healthy humans. *J Appl Physiol* 97: 797-805, 2004.

3. **Laurie SS BK, Yang X, Elliott JE, Lovering AT.** Identification of the threshold for hypoxia-induced intrapulmonary arteriovenous shunting in humans at rest, 2009.

4. **Laurie SS BK, Yang X, Elliott JE, Lovering AT. .** Hypoxia-induced intrapulmonary arteriovenous shunting increases over time in humans at rest, 2009.

5. **Loeppky JA IM, Charlton GA, Conn CA, Maes D, Riboni K, Gates L, Melo MF, Roach RC.** Hypoxemia and acute mountain sickness: which comes first? *High Alt Med Biol* 9: 271-279, 2008.

6. **Lovering AT, Haverkamp HC, and Eldridge MW.** Responses and limitations of the respiratory system to exercise. *Clin Chest Med* 26: 439-457, vi, 2005.

7. **Lovering AT LS, and Yang X.** Human Subjects Research Protocol Application 2008.

8. **Lovering AT, Romer LM, Haverkamp HC, Pegelow DF, Hokanson JS, and Eldridge MW.** Intrapulmonary shunting and pulmonary gas exchange during normoxic and hypoxic exercise in healthy humans. *J Appl Physiol* 104: 1418-1425, 2008.

9. **Lovering AT, Stickland MK, Amann M, Murphy JC, O'Brien MJ, Hokanson JS, and Eldridge MW.** Hyperoxia prevents exercise-induced intrapulmonary arteriovenous shunt in healthy humans. *J Physiol* 586: 4559-4565, 2008.

10. **Lovering AT, Stickland MK, and Eldridge MW.** Intrapulmonary shunt during normoxic and hypoxic exercise in healthy humans. *Adv Exp Med Biol* 588: 31-45, 2006.

11. **Lovering AT, Stickland MK, Kelso AJ, and Eldridge MW.** Direct demonstration of 25- and 50-microm arteriovenous pathways in healthy human and baboon lungs. *Am J Physiol Heart Circ Physiol* 292: H1777-1781, 2007.

12. **Lumb AB and Nunn JF.** *Nunn's applied respiratory physiology*. Edinburgh ; Philadelphia: Elsevier Butterworth Heinemann, 2005.

13. **McMullan DM, Hanley FL, Cohen GA, Portman MA, and Riemer RK.** Pulmonary arteriovenous shunting in the normal fetal lung. *J Am Coll Cardiol* 44: 1497-1500, 2004.

14. **Powers SK and Howley ET.** *Exercise physiology : theory and application to fitness and performance*. Boston: McGraw-Hill, 2007.

15. **Sedgewick J.** *Scientific imaging with Photoshop : methods, measurement, and output*. Berkeley, CA: New Riders, 2008.

16. **Shapiro RS, Wagreich J, Parsons RB, Stancato-Pasik A, Yeh HC, and Lao R.** Tissue harmonic imaging sonography: evaluation of image quality compared with conventional sonography. *AJR Am J Roentgenol* 171: 1203-1206, 1998.

17. **Shub C, Tajik AJ, Seward JB, and Dines DE.** Detecting intrapulmonary right-to-left shunt with contrast echocardiography. Observations in a patient with diffuse pulmonary arteriovenous fistulas. *Mayo Clin Proc* 51: 81-84, 1976.

18. **Silverthorn DU.** *Human physiology : an integrated approach*. San Francisco: Pearson/Benjamin Cummings, 2007.

19. **Stickland MK and Lovering AT.** Exercise-induced intrapulmonary arteriovenous shunting and pulmonary gas exchange. *Exerc Sport Sci Rev* 34: 99-106, 2006.

20. **Stickland MK, Lovering AT, and Eldridge MW.** Exercise-induced arteriovenous intrapulmonary shunting in dogs. *Am J Respir Crit Care Med* 176: 300-305, 2007.

21. **Tobin CE.** Arteriovenous shunts in the peropheral pulmonary circulation in the human lung. *Thorax* 21: 197-204, 1966.

22. **Tobin CE and Zariquiey MO.** Arteriovenous shunts in the human lung. *Proc Soc Exp Biol Med* 75: 827-829, 1950.